



Piezoelectric Aluminum Nitride Resonator for Oscillator

Olivier Mareschal, Sebastien Loiseau, Aurelien Fougerat, Laurie Valbin, Gaelle Bazin Lissorgues, Sébastien Saez, Christophe Dolabdjian, Rachid Bouregba, Gilles Poullain

► To cite this version:

Olivier Mareschal, Sebastien Loiseau, Aurelien Fougerat, Laurie Valbin, Gaelle Bazin Lissorgues, et al.. Piezoelectric Aluminum Nitride Resonator for Oscillator. IEEE Transactions on Ultrasonics, Ferroelectrics and Frequency Control, 2010, 57 (3), pp.513-517. <10.1109/TUFFC.2010.1441>. <hal-00989677>

HAL Id: hal-00989677

<https://hal.science/hal-00989677v1>

Submitted on 12 May 2014

HAL is a multi-disciplinary open access archive for the deposit and dissemination of scientific research documents, whether they are published or not. The documents may come from teaching and research institutions in France or abroad, or from public or private research centers.

L'archive ouverte pluridisciplinaire **HAL**, est destinée au dépôt et à la diffusion de documents scientifiques de niveau recherche, publiés ou non, émanant des établissements d'enseignement et de recherche français ou étrangers, des laboratoires publics ou privés.



HAL Authorization

Piezoelectric Aluminum Nitride Resonator for Oscillator

Olivier Mareschal, Sébastien Loiseau, Aurélien Fougerat, Laurie Valbin, Gaëlle Lissorgues, Sebastien Saez, Christophe Dolabdjian, Rachid Bouregba, and Gilles Poullain

Abstract—This work investigates properties of the thin film elongation acoustic resonator (TFEAR) operating at megahertz frequencies in air. This resonator is composed of a piezoelectric layer of AlN sandwiched between 2 Al electrodes. TFEAR works in the extensional mode excited via AlN d_{31} piezoelectric coefficient. A 3D finite element method (3D-FEM) analysis using ANSYS software has been performed to model static modal and harmonic behavior of the TFEAR. To consider insertion losses into the substrate, equivalent electrical models based on a modified Butterworth-Van Dyke (MBVD) circuit have been improved by adding extra dissipative elements. Thus, a whole model for the on-wafer characterization setup is given, allowing for automatic de-embedding of the present TFEAR equivalent circuit. Quality factors Q as high as 2500 in air have been recorded with motional resistance lower than 400 Ω . A first oscillator based on a TFEAR resonator was also designed and tested.

I. INTRODUCTION

IN the last few years, microelectromechanical-system (MEMS) technology integration for RF applications has become a new challenge. Several applications like universal serial bus (USB), radio frequency identification (RFID), or personal digital assistant (PDA) use classical quartz oscillators, typically millimeter sized. MEMS resonators are submillimeter sized. It is a low consumption component and integrated circuit compatible. The aim of the thin film elongation acoustic resonator (TFEAR) [1] is to become a low-cost alternative for quartz crystal resonators in the megahertz range. Indeed, the manufacturing of TFEAR needs only 5 masking steps. In addition, megahertz frequency electrostatic resonators have been presented in earlier papers [2], but most of those solutions operate in vacuum and need high-bias resonator voltage (≈ 5 to 100 V). The main advantages of piezoelectric resonators are their low driving voltage (25 mV for the TFEAR) and their good elongation linearity versus applied voltage. In this paper, we report on the fabrication process method,

modeling, and electrical characterization of a piezoelectric AlN resonator. It works in air and is fully adapted for oscillator circuit miniaturization. A first simple oscillator based on TFEAR will also be presented.

II. EXTENSIONAL MODE, MODELING AND DESIGN

A. Working Principle

TFEAR is an in-plane extensional mode resonator. It consists of a multilayer beam constituted of insulator, metal, piezoelectric, and metal materials. The piezoelectric layer is composed of AlN, which is a noncontaminant material and presents high acoustic wave velocity [3]. In opposition to bulk acoustic wave (BAW) [4] and surface acoustic wave (SAW) [5], which work in thickness and surface mode, respectively, the TFEAR is directly driven by the piezoelectric coefficient d_{31} of AlN. Therefore, an excitation voltage applied on the piezoelectric thin film allows beam elongation.

B. Design

A 3-D finite element method (3D-FEM) analysis using ANSYS software (ANSYS Inc., Canonsburg, PA) has been performed, taking into account the piezoelectricity properties of anisotropic materials. It allowed comparison of different designs and prediction of expected resonance frequencies. Fig. 1 shows the result of one modal solution of a FEM calculation for extensional mode along the beam. The simulation takes into account the piezoelectric layer, the electrodes, and the part of the substrate (Si) where the beam is anchored. The excitation voltage is applied on the Al electrode deposited on the whole piezoelectric layer, which induced a resonance. However, we noticed that, although ANSYS software allows us to evaluate the flexure mode, it appears in the kilohertz range, so the flexure mode has no influence on the electrical behavior of the extensional mode that works in the megahertz range. In this last case, the resonance frequency, for extensional mode, follows the well-known relation

$$f_r = \frac{1}{2L} \sqrt{\frac{\bar{E}}{\bar{\rho}}} \quad (1)$$

where L is the length of the beam, \bar{E} is equivalent Young modulus of the stacked layers, which does not depend on

Manuscript received May 19, 2009; accepted September 15, 2009.

O. Mareschal, S. Loiseau, and A. Fougerat are with NXP Semiconductors, Caen, France (e-mail: olivier.mareschal@greyc.ensicaen.fr).

O. Mareschal and G. Lissorgues are with ESYCOM, ESIEE Paris & Université Paris-Est, Noisy-le-Grand, France.

L. Valbin is with ESIEE, ESIEE Paris & Université Paris-Est, Noisy-le-Grand, France.

O. Mareschal, S. Saez, and C. Dolabdjian are with GREYC—CNRS UMR6072, ENSICAEN & Université de Caen Basse-Normandie, Caen, France.

S. Loiseau, R. Bouregba, and G. Poullain are with CRISMAT—CNRS UMR6508, ENSICAEN & Université de Caen Basse-Normandie, Caen, France.

Digital Object Identifier 10.1109/TUFFC.2010.1441

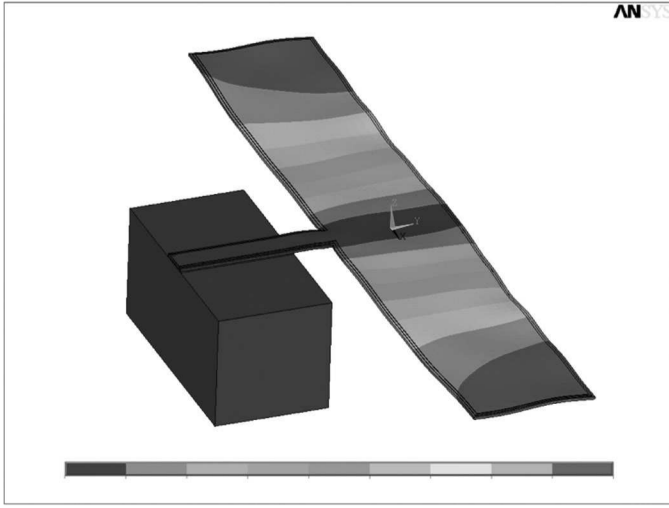


Fig. 1. 3D-finite element method result for extensional mode in ANSYS software modal analysis (continuous optical color spectrum indicates local beam amplitude deformation).

piezoelectric coefficient, and $\bar{\rho}$ is the beam equivalent density. These 2 properties are balanced with the thickness of each layer [6].

III. MANUFACTURING PROCESS

A. TFEAR Process

TFEAR is realized using conventional integrated circuit manufacturing tools. Fig. 2 presents a schematic process flow. The resonator is made on silicon wafers covered by oxide silicon (a). Pads and the bottom electrode ($\text{AlSi}_{1\%}\text{Cu}_{0.04\%}$) are deposited by DC-magnetron sputtering tool, shown in (b) and (c). Thereafter, the AlN layer is deposited by an Oerlikon-pulsed DC reactive sputtering in a nitrogen and argon atmosphere (Oerlikon clusterline 200, OC Oerlikon Management AG, Pfäffikon, Switzerland) (d). The top electrode is deposited in the same way as the bottom electrode (e). These 4 layers are patterned by dry etching for the $\text{AlSi}_{1\%}\text{Cu}_{0.04\%}$ and by wet etching for the AlN layer. Finally, TFEAR is released by designing of the cavity (f) using anisotropic and isotropic dry etching for the silicon oxide layer and the silicon substrate, respectively.

Fig. 3 shows a scanning electron microscopy view of the corresponding investigated resonator design in this paper (T-shaped anchor). The oxide layer is in compression regarding metal and piezoelectric layers. A TFEAR manufactured on the above conditions presents a seeming bent beam, which comes from the AlN and the SiO_2 known as a stressing layer. FEM simulations showed that stress in the beam does not change resonance frequency.

B. AlN Deposition

Regarding the piezoelectric AlN layer, underlayers had to be optimized to have the best crystallized mate-

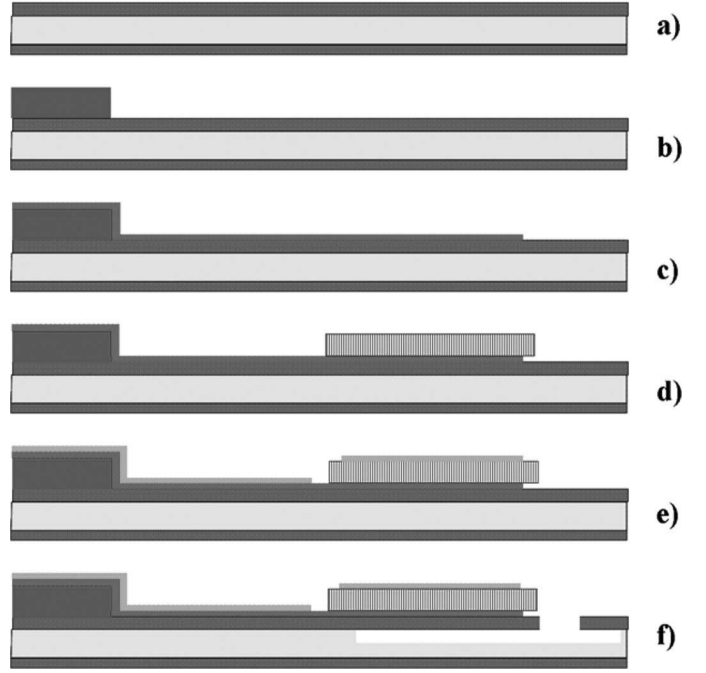


Fig. 2. Scanning electron microscopy view of a 275- μm long and 20- μm wide thin film elongation acoustic resonator.

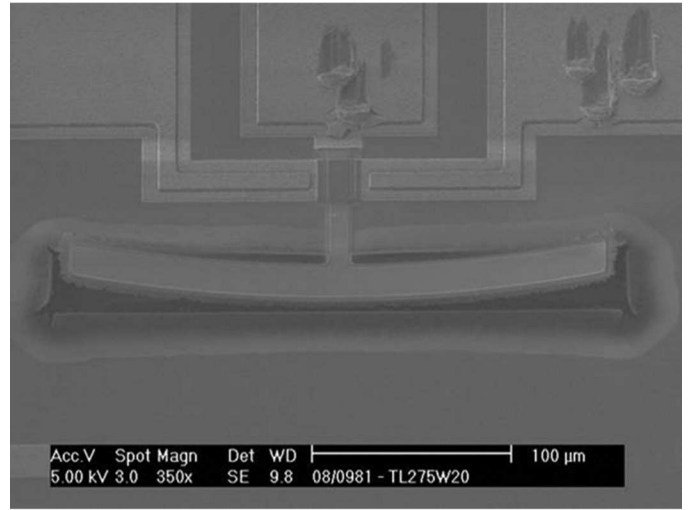


Fig. 3. Thin film elongation acoustic resonator cross-section process flow views.

rial. Then, experimental designs were used to optimize $\text{AlSi}_{1\%}\text{Cu}_{0.04\%}$ deposition parameters to get the highest crystallinity of AlN. Layers were characterized by X-ray diffraction (XRD). The best result obtained for the bottom electrode is shown in Fig. 4. A full width at half maximum (FWHM) of the rocking-curve equal to 4.78° was measured. The FWHM of the AlN film, prepared on this metal electrode and achieved by the Oerlikon sputtering tool, is presented in Fig. 5 ($\text{FWHM} = 2.18^\circ$). We noticed that the $\text{AlSi}_{1\%}\text{Cu}_{0.04\%}$ bottom electrode allows us to obtain a good crystalline quality of AlN, compared with previous studies [7]. The improvement of AlN layer deposition enabled us to obtain a high piezoelectric coef-

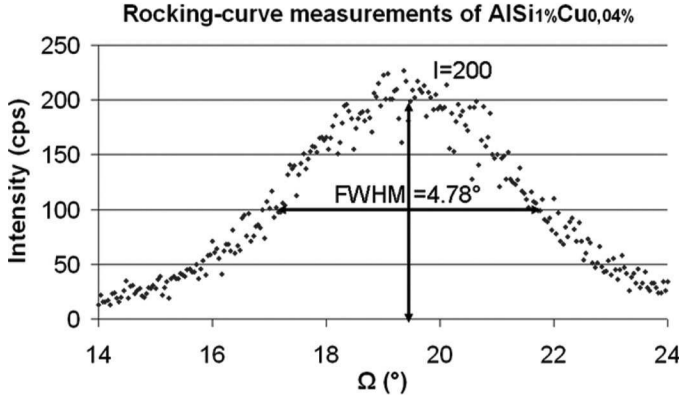


Fig. 4. X-ray of the rocking-curve for the bottom electrode.

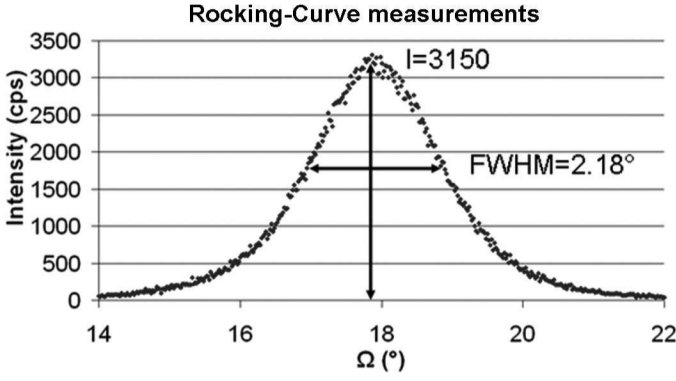


Fig. 5. X-ray of the rocking-curve for the AlN layer.

ficient and thus to maximize the quality factor Q of the resonator.

IV. EXPERIMENTAL RESULTS

A. MBDV Equivalent Circuit

The equivalent electrical model, based on Van-Dyke Butterworth circuit, was previously presented in an earlier paper [4]. The model used takes into account resistive and capacitive losses in the Si substrate, as summarized in Fig. 6.

During measurement, the wafer is connected to the ground. Therefore, the intrinsic resonator is parallel with the substrate parasitic equivalent elements. C'_0 corresponds to the capacitance of the resonator induced by both electrodes of the TFEAR (C_0), in parallel with the capacitance of the substrate. R'_p is the resistance of the AlN layer ($\approx G\Omega$) that is parallel with the resistance of the substrate. R_m , C_m , and L_m represent the motional arm of the Van-Dyke Butterworth model. The access line resistance and inductance are considered negligible in megahertz range TFEAR resonance frequency.

B. Electrical Properties and Physical Relationship

Fig. 7 gives the resonance frequency as a function of the inverse length of the TFEAR. We can observe the good

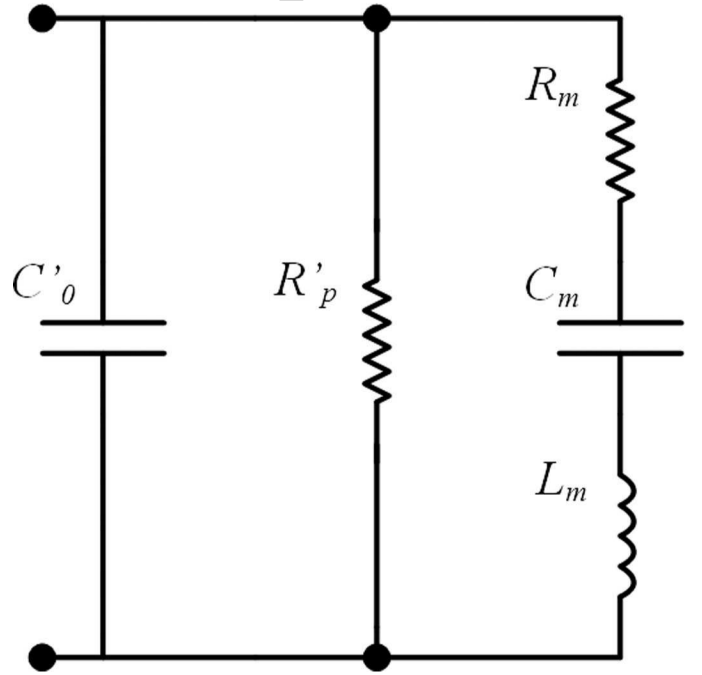


Fig. 6. Modified Butterworth-Van Dyke equivalent circuit of an effective 350- μm long and 50- μm wide thin film elongation acoustic resonator ($f_r = 14.35$ MHz, $C'_0 = 1.88$ pF, $R_{sp} = 9$ k Ω , $R_m = 375$ Ω , $C_m = 12.8$ fF, and $L_m = 9.6$ mH).

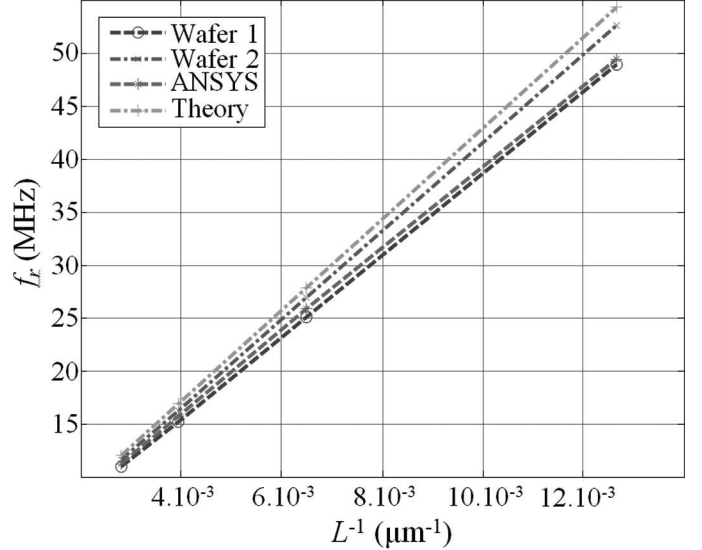


Fig. 7. Resonance frequency as a function of the resonator beam.

match between measurements made on 2 wafers, FEM simulation, and theory; compare (1). Discrepancies can be easily explained by fluctuations on the layer's thickness, which can occur during the process. In addition, for high frequency or low beam length, other resonance modes (e.g., contour mode) can be measured because the width is not negligible compared with the length of the beam. Presently, FEM simulation does not take into account the access line and substrate losses.

A basic relation gives the geometrical properties of the resonator versus the electrical parameters. Indeed, theory

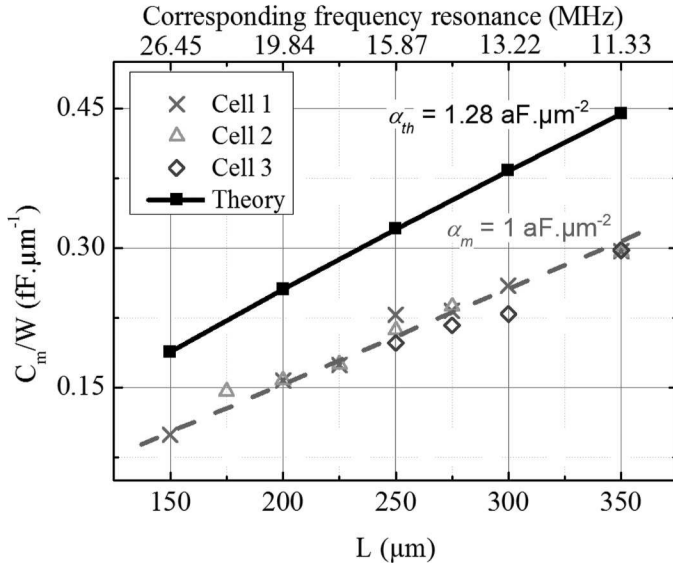


Fig. 8. Motional capacitance variation versus length of the thin film elongation acoustic resonator beam; α_{th} and α_m are theoretical and measured curve slopes, respectively.

shows that variations of motional capacitance and inductance are proportional to the length of the resonator beam according to the relations

$$C_m = \left[\left(\frac{f_a}{f_r} \right)^2 - 1 \right] C_0 = \alpha L W \quad (2)$$

and

$$L_m = \frac{1}{4\pi^2(f_a^2 - f_r^2)C_0} = \beta \frac{L}{W}, \quad (3)$$

where f_r and f_a are the resonant and antiresonant frequencies, respectively, α and β are 2 constants associated with materials (SiO₂, AlSiCu, and AlN) and layer thickness. C_0 is the capacitance of the resonator, fixed by the length, L , width, W , and thickness, t , of the TFEAR.

Figs. 8 and 9 show motional capacitance and motional inductance variations of the resonator versus the length of the TFEAR beam. The theoretical model is deduced from the differential equation governing the resonator without considering substrate losses. The cells correspond to measurement series for different devices made on the same wafer. Both figures show that there is no discrepancy for close resonators on the same wafer. In addition, the electrical parameter behavior is in good agreement with the theory and is being quite linear with similar slope. Measurements are normalized by C'_0 capacitance (and not by C_0), and the theoretical model does not take into account the SiO₂ layer and misalignment appearing during the process. This does not modify the linear behavior of the electrical parameters. However, they justify the shift between theoretical curve and measurements.

V. PERFORMANCES AND OSCILLATOR INTEGRATION

The fabricated resonator presents free beam length, which varies from 75 to 350 μm . It allows us to obtain

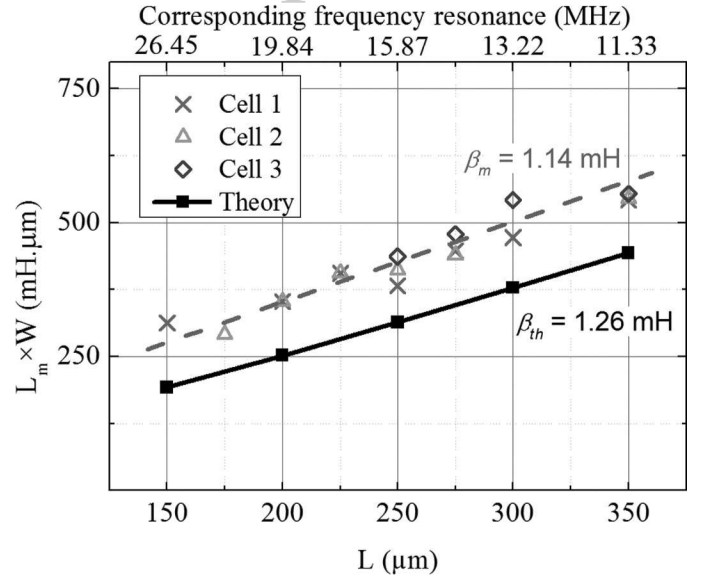


Fig. 9. Motional inductance variation versus length of the thin film elongation acoustic resonator beam; β_{th} and β_m are theoretical and measured curve slopes, respectively.

PERFORMANCES AND OSCILLATOR INTEGRATION

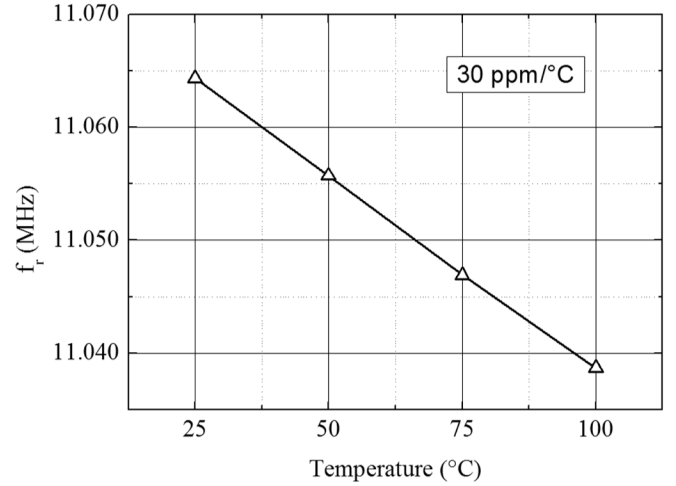


Fig. 10. Frequency shift versus temperature in uncompensated temperature mode ($f_{r0} = 11.06435$ MHz).

resonance frequencies f_r between 10 and 50 MHz according to (1). Quality factor Q as high as 2500 was measured [4] with motional resistance (R_m) of about 400 Ω . In uncompensated temperature mode (without SiO₂ layer), we recorded a frequency resonance accuracy of about 30 ppm/°C for 25 to 100°C temperature range; compare Fig. 10. Study is in progress to optimize the SiO₂ layer under the beam to decrease this value.

TFEAR was embedded in a simple oscillator circuit based on noninverting operational amplifier circuit. Fig. 11 shows the oscillogram obtained for a 325- μm long and 50- μm wide TFEAR. Expected theoretical resonance frequency of this resonator is about $f_r = 14.11$ MHz. It is in good agreement with the measured value ($f_{osc} \approx 14.13$ MHz).

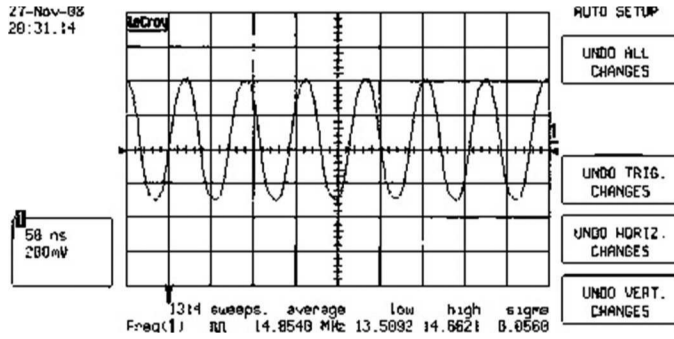


Fig. 11. Oscillogram of an oscillator output based on thin film elongation acoustic resonator.

VI. CONCLUSION

In this work, we have presented and characterized an in-plane extensional TFEAR. Resonance frequencies ranging from 10 to 50 MHz have been observed as expected. They are linked to TFEAR beam size, L , ranging from 75 to 350 μm , in our study. Simulation and measurement show good agreement with the theoretical model, which easily explains the electrical behavior of the resonator. In addition, basic relationships can be extracted from the model and data. A Q factor as high as 2500 and motional resistance below 400 Ω have allowed designing a first oscillator. This is the first step to specify the capability of the TFEAR to be embedded in industrial applications without significant change in classical existing oscillator cir-

cuits. Improvements on the process will allow us to obtain smaller motional resistance ($<100 \Omega$) and higher quality factor (>10000) to extend the compatibility of TFEAR in RF applications.

REFERENCES

- [1] T. T. Le, L. Valbin, F. Verjus, and T. Bourouina, "Micromachined piezoelectric resonator at MHz application," in *Proc. SPIE Smart Structures and Materials*, vol. 6172, 2006, art. no. 61720M.
- [2] C. T.-C. Nguyen, "MEMS technology for timing and frequency control," *IEEE Trans. Ultrason. Ferroelectr. Freq. Control*, vol. 54, pp. 251–270, Feb. 2007.
- [3] P. Muralt, J. Antifakos, M. Cantoni, R. Lanz, and F. Martin, "Is there a better material for thin film BAW applications than AlN?" in *Proc. IEEE Ultrasonics Symp.*, Rotterdam, The Netherlands, 2005, pp. 50–53.
- [4] M. A. Dubois, "Thin film bulk acoustic wave resonators: a technology overview," presented at MEMSWAVE 03, Toulouse, France, Jul. 2–4, 2003.
- [5] E. Benes, M. Groschl, F. Seifert, and A. Pohl, "Comparison between BAW and SAW sensor principles," *IEEE Trans. Ultrason. Ferroelectr. Freq. Control*, vol. 45, no. 5, pp. 1314–1330, Sep. 1998.
- [6] O. Mareschal, S. Loiseau, F. Verjus, L. Valbin, G. Lissorgues, R. Bouregba, G. Poullain, S. Saez, and C. Dolabdjian, "Modeling and fabrication of piezoelectric aluminum nitride resonator and its application in oscillators," *Proc. IEEE Transducers*, to be published.
- [7] M. Akiyama, K. Nagao, N. Ueno, H. Tateyama, and T. Yamada, "Influence of metal electrodes on crystal orientation of aluminum nitride thin films," *Vacuum*, vol. 74, no. 3–4, pp. 699–703, Jun. 2004.

Author photographs and biographies not available at time of publication.